INFN - Laboratori Nazionali di Frascati
Servizio Documentazione

LNF-91/052 (P)
12 Luglio 1991

The Intermediate Mass Higgs at LHC

G. Pancheri

Laboratori Nazionali di Frascati dell'INFN,
Frascati P.O.Box 13, 00044 Frascati ,Italy
PANCHERI@IRMLNF

Abstract

The search for the intermediate mass Higgs boson at the Large Hadron Collider is presented. Background processes and signals for the intermediate mass Higgs, i.e. one for which $m_W \leq m_H \leq 2m_W$ are discussed. It is pointed out that the search for Higgs bosons in the region around and just above the Z^0-mass puts very stringent limits on the detectors and that this region can be fully explored only with a very high luminosity option.

1 Introduction

In this talk I shall discuss rates and event signatures for intermediate Higgs boson searches at the Large hadron Collider (LHC) to be built in the LEP tunnel at CERN [1], in light of recent results from the CDF Collaboration [2] and from LEP [3] which have substantially restricted the range of variability in the Higgs and top mass values and thus allow for more precise predictions than the previous quite extensive studies[4].

At present, searches for the Higgs boson at LEP have established an important lower limit to the Higgs mass, i.e. $m_H \geq 49GeV$ [3]. It is expected that these limits can be extended by LEP200 to values close to the Z^0-mass, but probably not higher[5]. Were these searches to prove unsuccessful, the exploration of the higher mass region will be left to the hadron colliders[6] or to possible e^+e^- machines with c.m. energy of at least 400-500 GeV[7].

In principle, as we shall see, hadron colliders are able to explore a wide mass region, from m_Z up to 1 TeV. However, recent lower limits on the top mass from CDF Collaboration [2] have rendered this search more difficult, due to the the fact that previously background free channels, like for instance $H \rightarrow W^+W^-$, are now contaminated by strong production from $t\bar{t}$ pairs [1]. Because of the presence of this copious background from W-bosons of QCD origin, one is limited to observe Higgs decays into charged lepton pairs (from Z^0, on and off-the-mass-shell) or into photons, since these are the only decays which insure the necessary quality for signal identification. This of course implies a loss of signal, since W-channels and decay ratioes into leptons are higher than for Z^0's. In turn, this poses stringent limits to the luminosity requirements.

Since the coupling to fermion pairs is proportional to the Higgs mass, the physics of the SM Higgs strongly depends upon the value of the top quark mass. The fact that the this value is now higher than that of the W-boson determines very precisely all the branching ratioes of the light mass Higgs, which is almost completely decoupled from the top quark. The remaining dependence on the top mass, for Higgs bosons in the mass range $m_W \leq m_H \leq 2m_W$, is through the top quark contribution to higher loop effects. LEP results on the other hand also reduce the uncertainty on the branching ratioes of the heavier Higgs, since the top quark mass, through radiative corrections to the Electroweak Parameters[8],has now been restricted to be less than 200 GeV, at 95% C.L.

Sections 2 and 3 will be devoted to a general review of widths and production cross-sections for the Higgs boson. In section 4 a more detailed analysis of event signatures and backgrounds for the intermediate mass Higgs will be presented.

2 Decay Properties of the Higgs Boson

The Higgs boson decays into all known elementary particles, including gluons and photons, with these decay channels proceeding through higher order QCD and QED processes. One distinguishes 4 types of decay modes ,

$$H \rightarrow f\bar{f} \tag{2.1}$$

$$H \rightarrow gluon\ gluon \tag{2.2}$$

$$H \rightarrow \gamma\gamma \tag{2.3}$$

$$H \rightarrow V_1\ V_2 \tag{2.4}$$

which shall now be discussed in some detail.

2.1 Decay into a fermion pair

For decay into a fermion-antifermion pair, to lowest order in the coupling constants, the following expression [9] holds :

$$\Gamma_0(H \rightarrow f\bar{f}) = c_f \frac{G_F m_f^2 M_H}{4\pi\sqrt{2}} [1-\epsilon_f]^{3/2} \tag{2.1}$$

where $c_f = 1$ for leptons, $c_f = 3$ for quarks and $\epsilon_f = \frac{4m_f^2}{M_H^2}$ and $G_F = 1.166\text{x}10^{-5}\ GeV^{-2}$.

In the case of quarks, higher order QCD corrections modify this result[10, 11, 12]. The corrections come from virtual gluon exchanges as well as from soft and hard gluon emission. For $M_H >> m_f$, the overall correction is large and negative, so that the effective decay width into fermions is smaller than the one given by Eq. 2.1. An interpolating formula which connects the full one loop expression near threshold and the leading log result at large M_H, has been proposed by Drees and Hikasa [11] as follows :

$$\Gamma(H \rightarrow q\bar{q}) = \Gamma_0 \left(\frac{log(\frac{4m_q^2}{\Lambda^2})}{log(\frac{m_H^2}{\Lambda^2})} \right)^{24/(33-2N_f)} \left[1 + \frac{9}{4}\frac{C_F\alpha_s}{\pi}\right] \tag{2.2}$$

where Γ_0 is the Higgs boson width into $q\bar{q}$ pairs as calculated in zeroeth order in α_s, Eq. 2.1, N_f is the number of flavours, Λ is the QCD scale. Phenomenologically, we can take care of the largest part of the correction by simply replacing the quark mass parameter in Eq. 2.1 with the running quark mass, evaluated at $Q^2 = M_H^2$. In the Higgs mass region under consideration, this replacement amounts to have a mass parameter for the b-quark around 3 GeV.

For completeness we also discuss possible decays of the Higgs boson into virtual top-quark pairs, although this channel does not contribute significantly to the total width. The analytical expression for this process has been derived [16] and can be written as

$$\Gamma\left[H \rightarrow t^*\bar{t}^* \rightarrow (bf_1\bar{f}_2)(\bar{b}f_3\bar{f}_4)\right] = \int_{m_b^2}^{(m_H-m_b)^2} \frac{Q_1 dQ_1^2}{\pi} \frac{\Gamma(t^* \rightarrow bf_1\bar{f}_2)}{(Q_1^2-m_t^2)^2+(\Gamma_{t^*}m_t)^2} \cdot$$
$$\cdot \int_{m_b^2}^{(m_H-Q_1)^2} \frac{Q_2 dQ_2^2}{\pi} \frac{\Gamma(\bar{t}^* \rightarrow \bar{b}f_3\bar{f}_4)}{(Q_2^2-m_t^2)^2+(\Gamma_{\bar{t}^*}m_t)^2}\ \Gamma(H \rightarrow t^*\bar{t}^*) \tag{2.3}$$

where the width into both t and $\bar{t}$ off the mass shell is defined as

$$\Gamma(H \rightarrow t^*\bar{t}^*) = 3\frac{m_t^2 g_t^2}{8\pi m_H^3} \frac{\lambda^{1/2}(m_H^2, Q_1^2, Q_2^2)}{Q_1^2 Q_2^2} \cdot$$
$$\cdot \left[\frac{1}{2}m_H^2(Q_1^2+Q_2^2) - \frac{1}{2}(Q_1^2+Q_2^2)^2 - 2Q_1^2Q_2^2\right] \tag{2.4}$$

with $g_t = \frac{g}{2m_W}$, $g = \frac{e}{cos\theta_W}$. The decay width of an off-shell top quark of mass Q comparable to that of the W-boson has the form[13, 14, 15]

$$\Gamma_Q = 9\frac{G_F^2 m_W^4}{96\pi^3 Q^3} \int dk^2 \frac{\lambda^{1/2}(Q^2, m_b^2, k^2)}{(k^2-m_W^2)^2+\Gamma_W^2 m_W^2} [(Q^2-m_b^2)^2 + k^2(Q^2+m_b^2) - 2k^4] \tag{2.5}$$

Here we assume $\mid V_{tb} \mid = 1$. The factor 9 comes from summing all $W^* \rightarrow f\bar{f}'$ channels

neglecting final fermion masses and QCD corrections, and $\lambda(a,b,c) = a^2 + b^2 + c^2 - 2ab - 2ac - 2bc$.

In **Fig.1** we show the Higgs boson width into $b\bar{b}$ and $t\bar{t}$ pairs, as it obtained from Eqs. 2.1 and 2.4, for $m_t = 90, 200$ GeV and $m_b = 3, 5$ GeV.

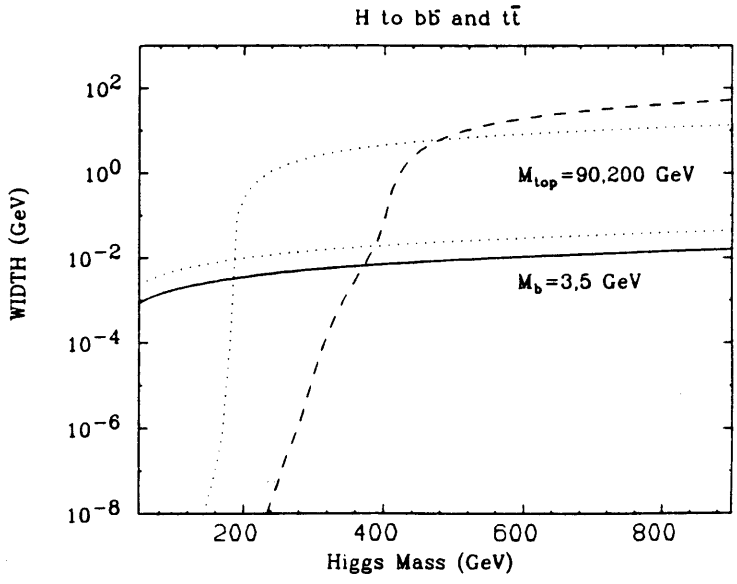

Fig. 1 Higgs boson decay width into $b\bar{b}$ and $t\bar{t}$ pairs.

2.2 Decay into Gluon Gluon

One has[17]

$$\Gamma(H \rightarrow gluon\ gluon) = \frac{G_F M_H^3}{4\pi\sqrt{2}} \left[\frac{\alpha_s(M_H^2)}{\pi}\right]^2 |\eta_{gg}|^2 \tag{2.6}$$

where

$$\eta_{gg} = \sum_i \eta_i = \sum_i \int_0^1 dx \int_0^{(1-x)} \frac{dy(1-4xy)}{1 - xyM^2/m_i^2 + i\epsilon} \tag{2.7}$$

and it corresponds to the Feynman diagram for the process

$$gluon\ gluon \rightarrow H$$

which proceeds through a closed triangle loop, getting contribution from all possible quark intermediate states. The function η is complex, in general and , for any given intermediate quark state, can be written as

$$\eta_i = \frac{\epsilon_i}{2}\left[1 + (\epsilon_i - 1)\phi(\epsilon_i)\right] \tag{2.8}$$

with $\epsilon_i = \frac{4m_i^2}{M_H^2}$ and with

$$\phi(\epsilon) = -\left[arcsin(\frac{1}{\sqrt{\epsilon}})\right]^2 \quad for\ \ M_H \leq 2m_i \tag{2.9}$$

and

$$\phi(\epsilon) = \frac{1}{4}\left[log\frac{1+\sqrt{1-\epsilon}}{1-\sqrt{1-\epsilon}} + i\pi\right]^2 \quad for \;\; M_H \geq 2m_i \tag{2.10}$$

In **Fig.2** we show a plot of the function $|\eta_i|^2$ vs.M_H for different values of the quark mass m_i. Notice that $\eta \rightarrow 0$ as the mass of the quark goes to zero, and that it reaches a constant value $|\eta|^2 \approx 0.1$ for large quark masses. We see from **Fig.2** that for a heavy Higgs a large value for the top mass would enhance the decay width into two gluons. The Higgs partial width into gluon-gluon is shown in **Fig. 3**.

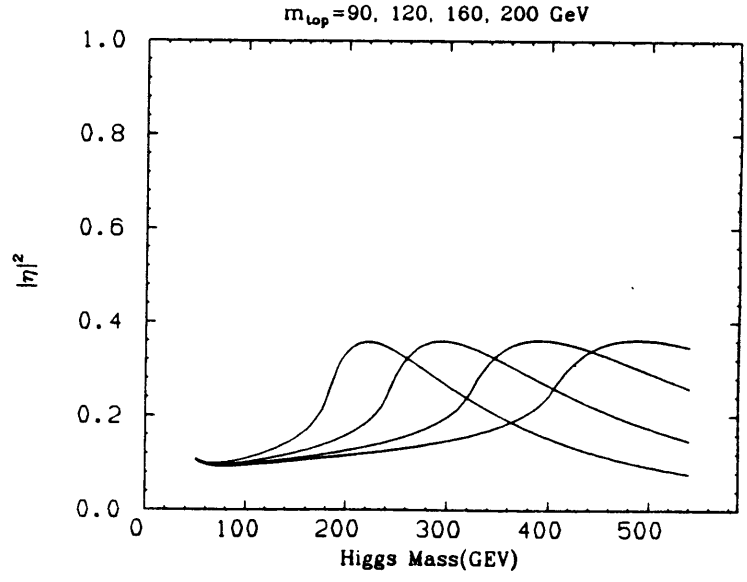

Fig. 2 Squared matrix element for *gluon gluon* $\rightarrow$ *Higgs* as a function of the Higgs boson mass for different top mass values.

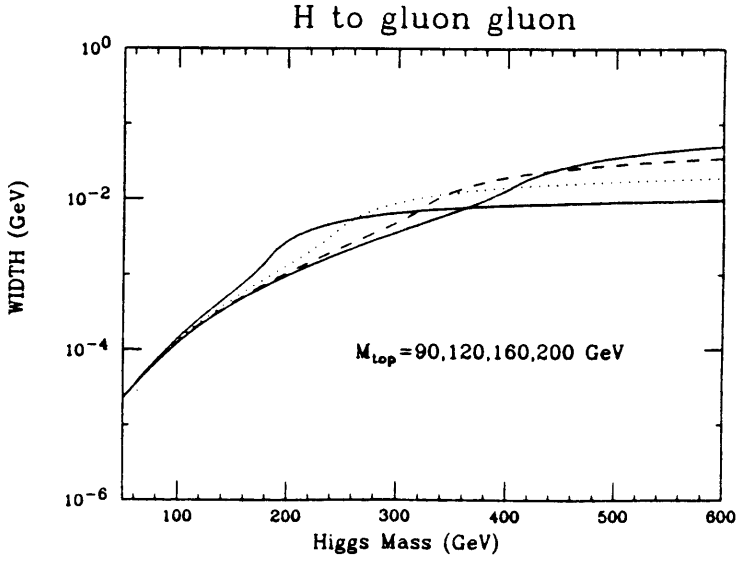

Fig. 3 Higgs boson decay width into gluon gluon.

2.3 Decay into $\gamma\gamma$

For the decay into photons[18],

$$\Gamma(H \to \gamma\gamma) = \frac{G_F M_H^3}{8\pi\sqrt{2}} \left[\frac{\alpha_s(M_H^2)}{\pi}\right]^2 |\eta_{\gamma\gamma}|^2 \tag{2.11}$$

where $\eta_{\gamma\gamma}$ now receives contributions from all existing intermediate charge states, quarks, leptons and W's. Due to the different couplings, these contributions have different expressions and even different signs, so that cancellations can and do occur, as we shall see below. One has

$$\eta_{\gamma\gamma} = 3\sum_q Q_q^2 \eta_q + \sum_l Q_l^2 \eta_l + \eta_W \tag{2.12}$$

where the indexes q and l run over all intermediate quark and lepton states with charges Q_q and Q_l respectively. η_k is defined as in Eq. 2.8, whereas

$$\eta_W = \frac{3\epsilon_W}{4}[(2-\epsilon_W)\phi(\epsilon_W) - 1] - \frac{1}{2} \tag{2.13}$$

with the function $\phi(\epsilon)$ as in Eq. 2.9.

Since fermions and bosons contribute with different signs to the decay amplitude of Higgs into photons, this width is not monotonically increasing with the Higgs mass, as one can see from **Fig.4** where the partial width into $\gamma\ \gamma$ is plotted for different top masses.The peculiar behaviour observed when the top mass is larger than the W-mass, is due to the presence of cancellations in the real and imaginary part of the function η between the fermionic and bosonic contributions. This can be seen in

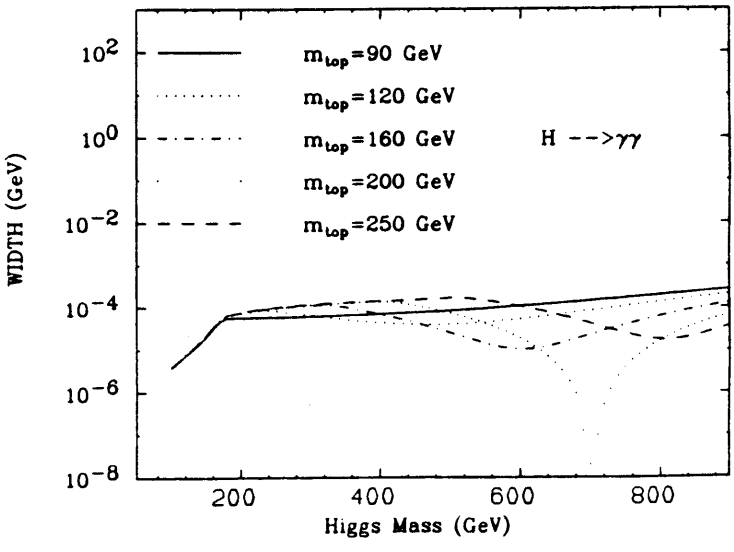

Fig. 4 Decay width of the Higgs boson into two photons for various values of the top quark mass, as indicated.

Figs. 5 and **6**, where we have plotted the real and imaginary parts of the functions $-\eta_W$, defined as in Eq. 2.8, and η_{top}, defined as

$$\eta_{top} = 3\,\frac{4}{9}\,\eta(\frac{4m_t^2}{M_H^2}) = \frac{2}{3}\epsilon_{top}[1 + (\epsilon_{top} - 1)\phi(\epsilon_{top})] \tag{2.14}$$

In these figures, the W-boson contribution appears as a full line, whereas the top contribution is either dots (m_{top} = 90 GeV) or dashes (m_{top} = 200 GeV). One notices that the top contribution is close (and opposite in sign) to that from the W both for the imaginary as well as for the real part only for a rather large top mass . For the lower top mass, the imaginary parts never cancel and thus the contribution to the loop remains finite.

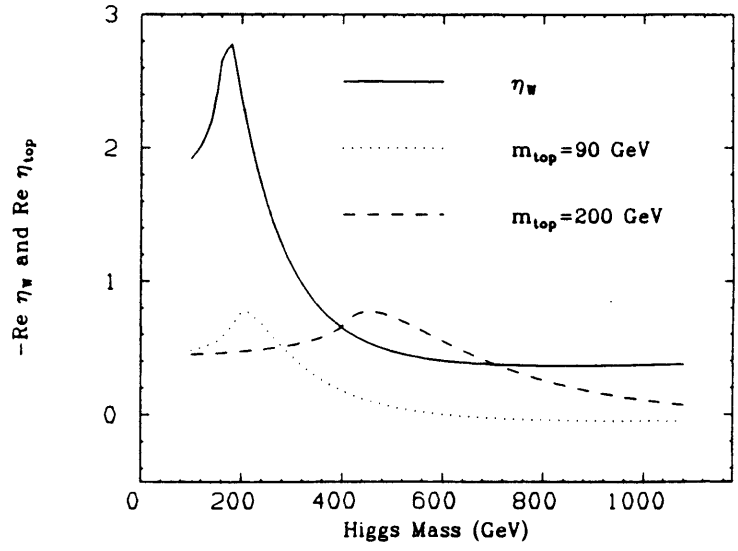

Fig. 5 *Re* η_{top} and $-Re\ \eta_W$ as defined in sect.2.2 as a function of the Higgs mass for two different values of the top mass. Cancellation between the real parts occurs for $M_{Higgs} \geq 2m_{top}$.

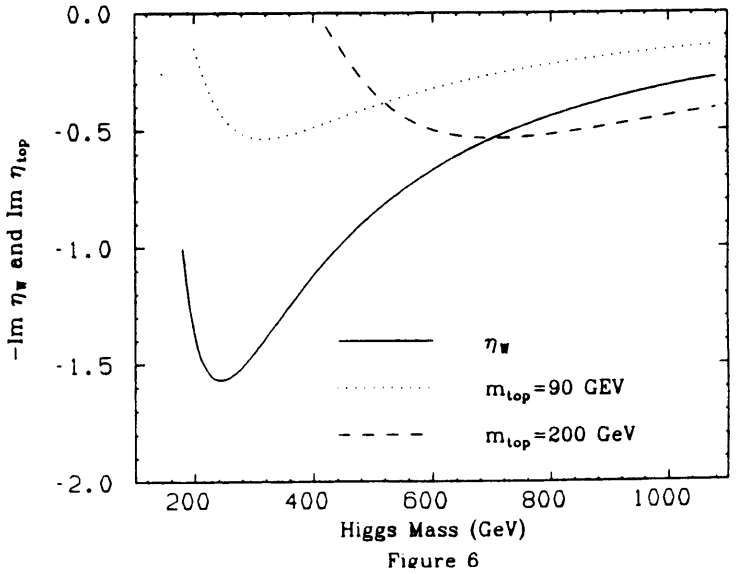

Figure 6

Fig. 6 As in Fig. 5 for the Imaginary parts.Since $Im\ \eta_{top} \neq 0$ only for $M_{Higgs} \geq 2m_{top}$, whereas $Im\ \eta_W \neq 0$ for all $M_{Higgs} \geq 2m_W$, total cancellation between real and imaginary parts occur for $m_{top} \cong 200$ GeV and $M_{Higgs} \approx 700$ GeV.

2.4 Decay into Vector Bosons with Discussion of $H \to 4\mu's$ below and around the 2 IVB's Threshold

Turning now to the vector bosons, one has[19]

$$\Gamma(H \to V_1 V_2) = C_V \frac{G_F M_H^3}{8\pi\sqrt{2}} (1 - \epsilon_V)^{1/2} \left(1 - \epsilon_V + 3\epsilon_V^2\right) \tag{2.15}$$

where $C_V = 1$ for W's and $C_V = \frac{1}{2}$ for Z_0's, because of the symmetrization of the final state for this latter case. Decay into vector bosons is the dominant decay channel for a Higgs boson heavier than twice the W-mass, whereas in the region below the 2 IVB threshold , the width is dominated by decay into $b\bar{b}$ pairs. The contribution of the top quark, for which the limit $m_{top} \geq 89\ GeV$ has been placed [2], enters only after the opening of the IVB channel. Notice in any case that , for large Higgs masses $M_H > m_{top}$, the decay into $t\bar{t}$ is relatively less important than that into IVB pairs. In fact, while the width into the vector boson increases like $\frac{M_H^3}{m_W^3}$, that into fermions only increases as $\left(\frac{m_f}{m_W}\right)^2 M_H$.

It has been noticed[1] that decay into vector boson pairs is relevant even for Higgs bosons in a mass range for which $M_H \leq 2m_W$. Indeed large QCD backgrounds make mandatory the selection of rare decay channels, namely photons and leptons, since these are the ones which can offer the cleanest experimental signature, although this will need to be paid off through a very high price in luminosity.

We now examine in some detail the characteristic signal

$$H \to Z_0^* Z_0^* \to (\mu^+\mu^-)(\mu^+\mu^-) \tag{2.16}$$

where Z_0^* is a neutral vector boson off-mass-shell.This decay can give a discernible signal for $M_H \approx 130 \div 200\ GeV$. In this region, the decay of eq. 2.16 proceeds through one real and one virtual Z_0 emission.To see this most clearly, let us first examine the overall decay width for one or both Z_0 off-the-mass shell. The decay width for the process

$$H \to Z_0(Z_0^* \to\ all\ decay\ products) \tag{2.17}$$

has been calculated by Keung and Marciano [20].

Their expression does not take into consideration finite width effects, and does not extrapolate below the one IVB threshold. To extend it both towards the upper and the lower end of the interesting Higgs mass values, we present here an expression in which both IVB's are off-the-mass shell.

If one is only interested in the invariant mass distributions, the calculation is very much simplified. In this case, the differential decay probability for the process (2.16) can be written as [16]

$$\frac{d\Gamma(H \to Z^* Z^*)}{dQ_1^2 dQ_2^2} = \frac{m_Z \Gamma_Z}{\pi\left[(Q_1^2 - m_Z^2)^2 + (m_Z\Gamma_Z)^2\right]} \cdot$$
$$\cdot \frac{m_Z\ \Gamma_Z}{\pi\left[(Q_2^2 - m_Z^2)^2 + (m_Z\Gamma_Z)^2\right]} \Gamma(H \to Z^* Z^*) \tag{2.18}$$

where $\Gamma(H \to Z^* Z^*)$ represents the decay width of a Higgs Boson into a pair of virtual bosons of masses Q_1 and Q_2 and it is given by

$$\Gamma(H \to Z^* Z^*) = \frac{G_F m_H^3}{16\pi\sqrt{2}} \Lambda^{1/2}(1,\lambda_1,\lambda_2)\,(1+\lambda_1^2+\lambda_2^2+10\lambda_1\lambda_2-2\lambda_1-2\lambda_2) \quad (2.19)$$

with $\lambda_i = \frac{Q_i^2}{m_H^2}$ and $\Lambda(a,b,c) = a^2+b^2+c^2-2ab-2ac-2bc$.

The expression for $d\Gamma$ can also be written as[21]

$$d\Gamma(H \to_0 Z^* Z_0^*) = \frac{\epsilon^2}{8\pi^3\omega}\frac{G_F M_Z^3}{\sqrt{2}} dx_1 dx_2 \left[\frac{\omega^2 - 2\omega(x_1+x_2)+(x_1-x_2)^2}{4\omega}\right]^{1/2} \cdot$$

$$\cdot\, x_1 x_2 \;\frac{\gamma^2\gamma'^2[10(1+\beta\beta')^2 - 6(\beta+\beta')^2]+2}{[(x_1-1)^2+\epsilon^2]\;[(x_2-1)^2+\epsilon^2]} \quad (2.20)$$

with $x_i^2 = Q_i^2/M_Z^2$, $\omega = m_H^2/M_Z^2$, $\epsilon = \Gamma_Z/M_Z$, and

$$\gamma^2 = \frac{(m_H^2+Q_1^2-Q_2^2)^2}{4m_H^2 Q_1^2} \qquad \beta^2 = 1-1/\gamma^2$$

$$\gamma'^2 = \frac{(m_H^2+Q_2^2-Q_1^2)^2}{4m_H^2 Q_2^2} \qquad \beta'^2 = 1-1/\gamma'^2$$

One then obtains

$$\Gamma(H \to all\ Z_0 Z_0) = \int_0^{m_H^2} dQ_1^2 \int_0^{(m_H-Q_1)^2} dQ_2^2 \frac{d\Gamma(H \to Z_0^* Z_0^*)}{dQ_1^2 dQ_2^2} \quad (2.21)$$

Eq. 2.21 is a convenient way to write the width, since it easily gives the expression for $H \to Z_0 Z_0$, when the narrow width approximation is used. The expression we have obtained agrees with the one obtained by Keung and Marciano, in the region $M_H \geq m_W$. Notice that, whenever phase space allows it, one of the two bosons will always be on the mass shell.

Before proceeding to a more detailed description of the use of Eq. 2.21, we shall compare width and branching ratioes for this process with other important processes, like decay into photons and leptons or into $t\bar{t}$. This will give an estimate of how large this process is. We show this comparison in **Fig.7**, where we have plotted the decay width into the IVB's, the width into $t\bar{t}$ for $m_{top} = 90$ and other channels of interest. From this figure one immediately obtains the branching ratioes. Since we are here interested in decay into lepton pairs, we have chosen to show the branching ratio of Higgs not into two Z^0's , but into two $\mu^+\mu^-$ pairs into which the Z^0 can eventually be detected. This of course lowers the branching ratio by a factor 10^{-3}. Width and branching fractions depend upon the value chosen for the mass of the heaviest quark below the W-mass, namely the b-quark. To incorporate the discussion of section 2.1, and leave space to a possible theoretical uncertainty, we have used Eq. 2.1 for the width into $b\bar{b}$ and have varied the b-mass between 3 and 5 GeV. We show in **Fig.8** the branching ratioes for Higgs into $\gamma\gamma$, $\mu^+\mu^-$ and $e^+e^-e^+e^-$'s in the range $50 \div 300\ GeV$. We see that the $\gamma-\gamma$ channel is dominant until $\approx 140\ GeV$, after which the decay into one real and one virtual Z^0 takes over.

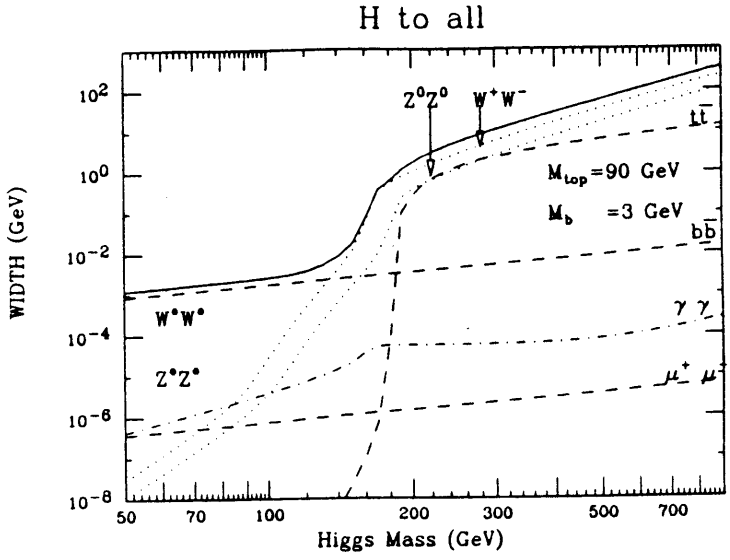

Fig. 7 Total Decay width of the Higgs boson (full line)and partial widths into : W^+W^- (dots), Z^0Z^0 (dots), $t\bar{t}, b\bar{b}, \gamma\gamma$ and $\mu^+\mu^-$. Formulae for off-mass-shell production have been used for all the channels indicated.

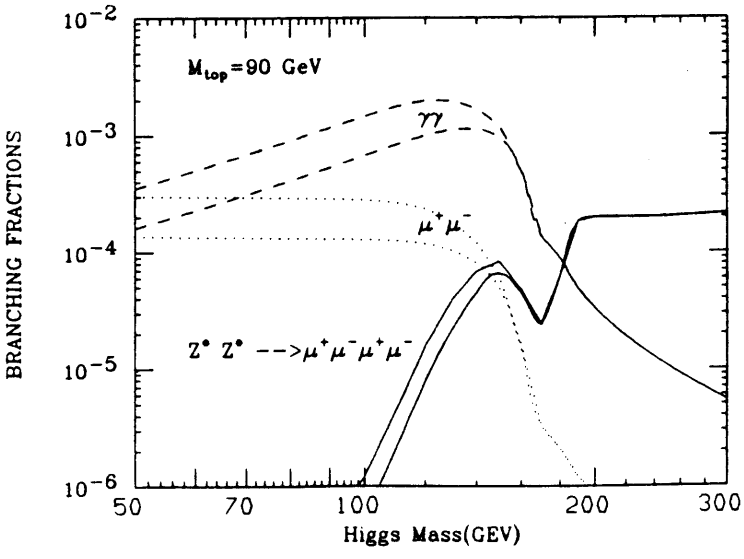

Fig. 8 Branching fraction for Higgs decay into : two photons (dashes), $\mu^+\mu^-$ (dots), 2 μ-pairs from $H \rightarrow Z_0^* Z_0^*$ (full line). Areas in between curves correspond to 3 $GeV \leq m_b \leq 5$ GeV. Top quark mass is 90 GeV.

3 Higgs Production Cross-Section at Hadronic Colliders

Direct production of the Higgs boson at hadronic colliders proceeds via the following three processes :

$$pp \rightarrow q\bar{q} + X \rightarrow H + X \tag{3.1}$$

$$pp \rightarrow gluon\ gluon\ + X \rightarrow H + X \tag{3.2}$$

$$pp \rightarrow V\ \bar{V} + X \rightarrow H + X \tag{3.3}$$

where V represents either a W or a Z_0. In addition, one can produce Higgs bosons in association with vector bosons, i.e. in processes like

$$pp \to q\bar{q} + X \to Z^*/W^* + X \to Z/W + H + X \tag{3.4}$$

We shall examine these processes separately and discuss briefly their properties. Notice that, unless otherwise indficated, all the cross-sections have been calculated using EHLQ [22] parton densities, set 2.

3.1 Direct Production through $q\bar{q}$ annihilation

Of the above, process (3.1) proceeds through the usual direct coupling of Higgs to the fermions and the cross section is given by

$$\sigma(a\ b \to q\bar{q} + X \to H + X) = \frac{G_F\pi}{3\sqrt{2}} \sum_i \frac{m_i^2}{M_H^2} \tau \frac{dL_{ii}}{d\tau} \tag{3.5}$$

where m_i is the mass of a quark of type i and the parton-parton luminosity function is defined as

$$\tau \frac{dL_{ij}}{d\tau} = \frac{\tau}{1+\delta_{ij}} \int_\tau^1 \frac{dx}{x} \left[f_i^a(x,Q^2) f_j^{(b)}(\frac{\tau}{x},Q^2) + f_i^b(x,Q^2) f_j^{(a)}(\frac{\tau}{x},Q^2) \right] \tag{3.6}$$

As we shall see more in detail in the following, the smallness of the quark masses renders this production mechanism less important than both gluon-gluon and IVB fusion.

3.2 Direct production through gluon gluon fusion

The most important contribution to Higgs production in the range below 1 TeV comes from gluon-gluon fusion. The integrated cross section for this process can be written as

$$\sigma(a\ b \to g\ g + X \to H + X) = \frac{G_F\pi}{32\sqrt{2}} \left[\frac{\alpha_s}{\pi}\right]^2 |\eta_{gg}|^2 \tau \frac{dL_{gg}}{d\tau} \tag{3.7}$$

where η_{gg} is defined as in Eq. 2.8. We already noticed that a large value for the top mass would enhance the coupling and hence production cross section for heavy Higgs. This is shown in **Fig.9** where the production cross-section for the Higgs boson through gluon-gluon fusion is presented.

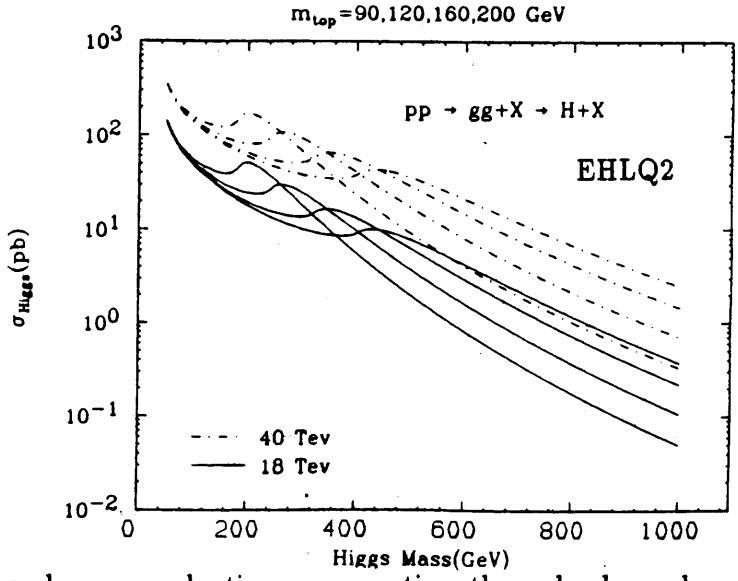

Fig. 9 Higgs boson production cross-section through gluon-gluon fusion at proton-proton colliders with $\sqrt{s}$ = 18, 40 GeV for different top mass values

3.3 Direct Production through IVB fusion

Another mechanism for Higgs production which can become important if the Higgs boson is heavier than the IVB's, is given by process 3.3, i.e. WW fusion or ZZ fusion[23, 24]. In evaluating the relative cross sections, use is made of the effective W-approximation , extending the parton model to include W and Z as partons in the protons. One can then define WW-luminosities, not unlike the case of gluon-gluon luminosities in hadronic collisions or photon-photon luminosities in electron-positron scattering. There are however important differences, due to the presence, for the W and Z case, of transversal and longitudinal components . There are theoretical uncertainties in defining separate luminosities for transversal and longitudinal W and the definition may depend upon the particular processes in which the W's scatter. There are basically three approximations which are usually done in order to simplify the calculation :

- (i) a small angle approximation, in which one assumes that the vector bosons are emitted at very small angles relative to the emitting quarks , and this is the basis of the effective W-approximation ;
- (ii) neglect of the interference between transverse and longitudinal cross-sections which allows to define separate transverse and longitudinal luminosities. This is justified for all those processes in which one mode is much more important than the other, as it iis the case for the production of a heavy Higgs boson coupling to the longitudinal modes.
- (iii) for very high energies, the rather cumbersome expression for the longitudinal density in a quark is approximated as follows

$$f_{q/V_{long}}(x) \approx \frac{C_{iV}^2 + C_{iA}^2}{4\pi^2} \frac{1-x}{x} \tag{3.8}$$

where C_{iV} and C_{iA} are the usual vector and axial couplings of the quarks to the vector bosons.

Presently, for the case of Higgs production and for large Higgs masses,i.e. $M_H \gg m_W$, the above approximations lead to a rather simple expression for the longitudinal luminosity of the two vector bosons,i.e.

$$\frac{dL}{d\tau}_{V_L V_L \ inpp} = \sum_{i,j} \int_\tau^1 \frac{dt}{t} \int_t^1 \frac{dx}{x} q_i(x,Q^2) q_j(\frac{t}{x},Q^2)$$

$$\left(\frac{C_{iV}^2 + C_{iA}^2}{4\pi^2}\right)\left(\frac{C_{jV}^2 + C_{jA}^2}{4\pi^2}\right) \frac{1}{\theta}[(1+\theta)log(1/\theta) + 2(1-\theta)] \quad \theta = \frac{t}{\tau} \tag{3.9}$$

Notice that these luminosities are independent of the center of mass energy $\sqrt{s}$, if the QCD scale is chosen to be $Q^2 = m_W^2$, as advocated by some authors. Their justification for this choice lies in the fact that the higher order graphs which are usually responsible for the Q^2-evolution of the parton densities are not ultraviolet divergent, in this case. Moreover, the proton only knows of the W-mass and of no other scale.

Within the parton model approximation, one can then write, as usual ,

$$\sigma(a\ b \to W^+\ W^- + X \to H + X) = \frac{\alpha\pi^2}{x_W m_W^2} \tau \frac{dL_{WW}}{d\tau} \tag{3.10}$$

We are now ready to combine the above production processes to obtain the overall cross-section for direct production of the Higgs boson . This is shown in **Fig. 10** where we have included the q-qbar cross-section calculated at the value m_{top}=30 GeV.However, this value is unrealistic . Notice that while the coupling to the Higgs boson tends to increase the $q\ \bar{q}$ contribution to the cross-section for large top masses,

the usual $\frac{1}{\hat{s}}$ dependence of the parton-parton cross-sections will decrease it, so that we do not expect this term to overcome the other two. We notice from this figure that present limits on the top mass, it is only when the Higgs mass is around 1 TeV, that WW-fusion can overcome gluon-gluon processes.

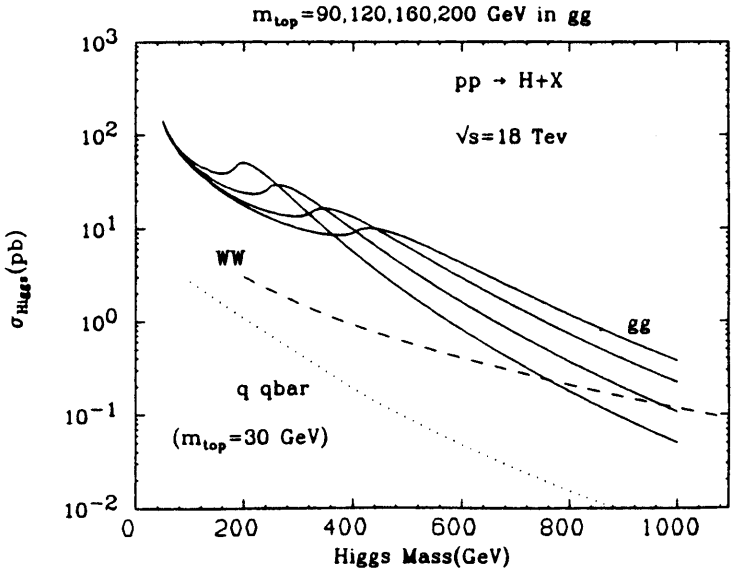

Fig. 10 Higgs production cross-section through different mechanisms as a function of the Higgs mass, at proton-proton colliders with $\sqrt{s} = 18$: gluon gluon fusion (full line) with $m_{top} = 90, 120$ GeV, WW fusion (dashes), quark-antiquark annihilation with a top quark of mass $m_{top} = 30$ GeV (dots).

3.4 Associated Production of Higgs and W/Z Bosons

In addition to direct Higgs production through $q\bar{q}$ or gluon-gluon fusion, the Higgs boson can be radiated from a vector boson, either a $W^{\pm}$ or a Z_0, through the so called Bjorken process [25] or from a top quark. These processes have a smaller cross-section than the ones which have been discussed previously, but they may offer clearer signals [26] (for the case of associated HV production) or additional evidence[27] (for the case $Ht\bar{t}$ production) for detection of a light-to-intermediate mass Higgs.

In the case of associated production with an IVB, the Higgs boson is always produced in association with a Z_0 or a W, which can be used to trigger the process. The cross-section for these processes can be written as

$$\frac{d\sigma}{dM}(ab \rightarrow HZ/W + X) =$$

$$\frac{2M}{s}\sum_{ij}\int_{-Y}^{Y} dy \left[f_i^a(x_a, M^2) f_j^{(b)}(x_b, M^2) + f_i^b(x_b, M^2) f_j^{(a)}(x_a, M^2)\right] \int_{-z_1}^{z_0} dz \frac{d\hat{\sigma}}{dz} \quad (3.11)$$

where M is the invariant mass of the WH or ZH system, and the parton parton cross-sections for production of an-off-shell IVB radiating a Higgs boson are given by

$$\frac{d\hat{\sigma}}{dz}(q_i\bar{q}_j \rightarrow HW^{\pm}) = \frac{\alpha^2 |U_{ij}|^2}{24\pi x_W^2}\left[\frac{2p^*}{\sqrt{(\hat{s})}}\right]\frac{1}{(\hat{s} - m_W^2)^2}\left(m_W^2 + \frac{p^{*2}}{2}(1 - z^2)\right) \quad (3.12)$$

and

$$\frac{d\hat{\sigma}}{dz}(q_i\bar{q}_i \to HZ) = \frac{\alpha^2(L_i^2+R_i^2)}{48\pi x_W^2(1-x_w)^2}\left[\frac{2p^*}{\sqrt{(\hat{s})}}\right]\frac{1}{(\hat{s}-M_Z^2)^2}\left(M_Z^2+\frac{p^{*2}}{2}(1-z^2)\right) \quad (3.13)$$

where z is the parton-parton center of mass scattering angle, p^* the c.m. momentum, $x_W = sin^2\theta_w$, U_{ij} the relevant KM matrix element, L_i and R_i are the chiral couplings of the neutral current, defined as

$$L_q = \tau_3 - 2Qx_w \qquad R_q = -2Qx_w$$

Q and τ_3 being respectively the charge and weak isospin projection of the quarks. In Eq.(3.12) the integration limits z_0 and z_1 depend on the rapidity cuts , so that if we impose that both final state bosons are produced with rapidity less than y_{cut}, one has

$$z_1 = \min\left[1, \beta_2^{-1}\tanh(y_{cut}-|y|), \beta_1^{-1}\tanh(y_{cut}+|y|)\right], \quad (3.14)$$

$$z_0 = \min\left[1, \beta_1^{-1}\tanh(y_{cut}-|y|)\right], \quad \text{for } |y_Z| \text{ or } |y_H| \leq y_{cut}$$

and

$$\beta_1 = \frac{p^*}{E_H}, \qquad \beta_2 = \frac{p^*}{E_{IVB}} \quad (3.15)$$

E_H and E_{IVB} being the energies of the final state bosons in the parton-parton cm system.

Of particular interest, although at the expense of a reduction in rate, is the process

$$pp \to Z^* + X \to ZH + X \quad (3.16)$$

because of the possibility of triggering on the Z_0 boson, a situation which offers a very clear signal. In **Figs.11** we show the total cross-section for HZ associated production, in comparison with a variety of other processes, all of which may contain a vector boson[28]. As mentioned this cross-section is lowest, but as we shall try to show later, comparison with various irreduble backgrounds is in favor of such a process. We also show in **Fig.12** a direct comparison of the cross-section between LHC ($\sqrt{s} = 16\ TeV$) and SSC ($\sqrt{s} = 40\ TeV$)

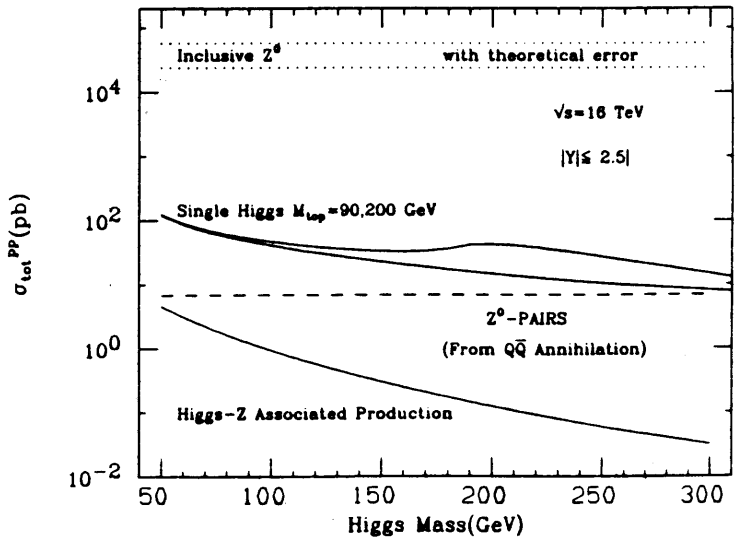

Fig. 11 Total cross-sections in p-p colliders, √s=16 TeV for: inclusive Z_0 production, single Higgs production from g-g fusion $|y_{Higgs}|\leq 2.5$, Z_0-pair production from qq annihilation $|y_{Z_0}|\leq 2.5$, associated production of Higgs and Z_0, both bosons with $|y|\leq 2.5$

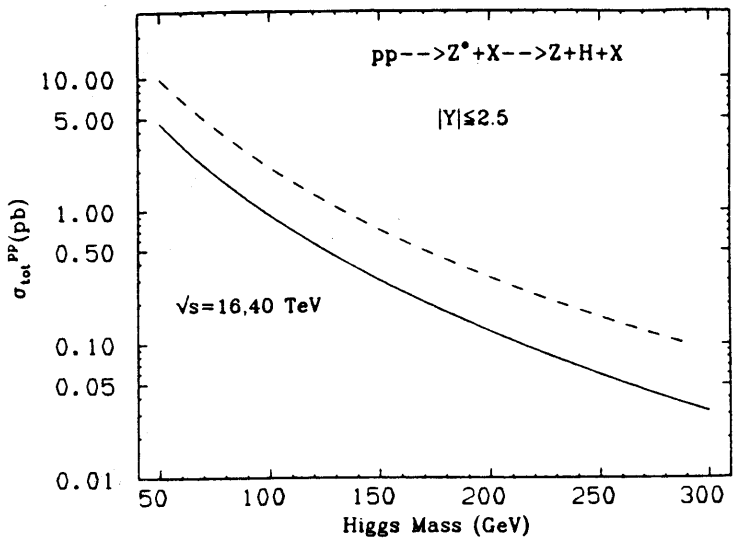

Fig. 12 Total cross-section for Higgs-Z^0 associated production as a function of the Higgs boson mass at $\sqrt{s} = 16, 40$ TeV.

4 Event Signatures and Background in the Intermediate Mass Region

In what follows we shall combine production cross-sections and branching fractions to discuss detectability of the Higgs boson and its discovery potential in specific channels. We limit ourselves to the the case in which the Higgs boson decays in leptons and photons, since these are the channels which offer the cleanest experimental signatures, albeit at the expense of a sever reduction in event rate.

We concentrate our attention to the region

$$m_W \leq M_H \leq 2m_Z$$

since it is expected that if a Higgs bosons lighter than the W-boson exists, it can be discovered in e^+e^- collisions when LEP energy will be raised to 100 GeV per beam. On the other hand, if the Higgs boson were substantially heavier than the W-boson, close to the TeV scale say, it could not be treated any more as a standard resonance. The study of the mechanism of electroweak symmetry breaking would then become of a more speculative nature[29, 30]with a scope outside the limits of the present work. Finally, the region between $3 \div 4$ m_W and the TeV scale has been extensively studied in the literature and the relevant material can be found in [31].

Because we limit ourselves to an intermediate, "standard" Higgs, we shall ignore the contribution of Vector Boson fusion, i.e. process (3.3) and only concentrate on direct Higgs production through gluon-gluon fusion or associated Higgs production in $q - \bar{q}$ annihilation. We also neglect the contribution of direct production through quark annihilation, which, in the region of interest in this note, is too small to play any relevant role.

This means that from now on we shall concentrate on discussing event rates and background contribution to the following processes

$$pp \rightarrow gg + X \rightarrow H + X \rightarrow \mu^+\mu^- + X \qquad (4.1)$$

$$pp \rightarrow gg + X \rightarrow H + X \rightarrow \gamma\gamma + X \quad (4.2)$$

$$pp \rightarrow gg + X \rightarrow H + X \rightarrow Z_0^* Z_0^* + X \rightarrow l_1^+ l_2^- l_3^+ l_4^- + X \quad (4.3)$$

$$pp \rightarrow q\bar{q} + X \rightarrow Z_0^* + X \rightarrow Z_0 + H + X \rightarrow l_1^+ l_2^- \gamma\gamma + X \quad (4.4)$$

Before discussing in detail event rates and background for the above processes, we show in **Fig.13** the different production cross-sections, in order to emphasize their relative importance. We shall now discuss the above processes one by one, starting from the first three, which proceed via direct Higgs production from gluon fusion.

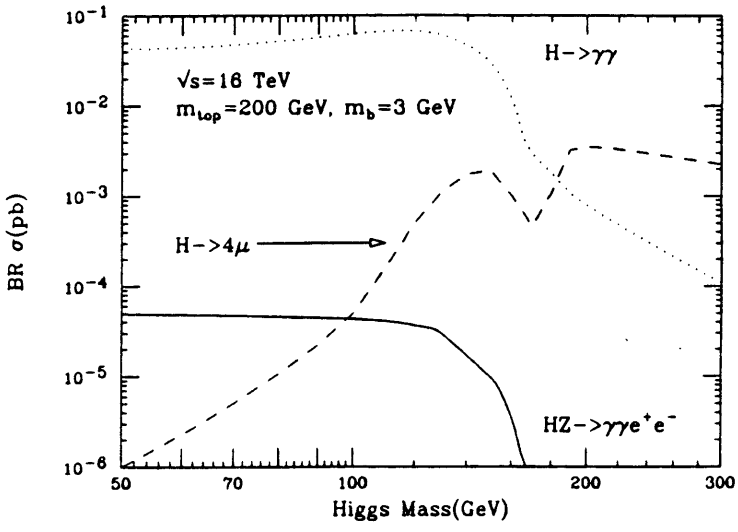

Fig.13 Total cross-section for Higgs production (direct and Z_0-associated) in some selected channels,with $|y_H| \leq 2.5|$ and no other cuts.

4.1 $H \rightarrow \mu^+\mu^-$

For Higgs bosons with a mass below the two IVB threshold, decay into a μ-pair is smaller than that into photons, but still larger , in certain mass regions, than the one into two μ-pairs. It is therefore of interest to investigate as to whether this process is a good candidate for Higgs search in the low-mass region. By folding the production cross-section with the branching ratio, we obtain a non-negligible cross-section, with a number of events certainly adequate for discovery. We show in **Fig. 14** number of events as a function of the Higgs mass. The number of events is calculated assuming a luminosity of $4 \times 10^{34} cm^{-2} sec^{-1}$ at the LHC , with a standard year of running time, i.e. $1y = 10^7 sec$.

The relevant physics background in this case is given by the production of μ-pairs from Drell-Yan and Z_0 production. Unfortunately this background turns out to be rather large for a low-to-intermediate mass Higgs. To compare the signal with the background, it should be noticed that below the two IVB's threshold, the Higgs boson is quite narrow with a width certainly below the experimental resolution. The signal would then appear as a peak inside a bin of width ΔE around the Higgs - mass value. We show in **Fig. 15** the invariant mass spectrum of a μ-pair from$\gamma - Z$ exchange together with the Higgs signal, at its peak value, divided by an assumed experimental resolution of 5 and 10 GeV, respectively. As mentioned, the signal is hopelessly below the background.

It should be noticed that there are many processes which can produce a μpair

with rather large invariant mass, notably strong production of $b\bar{b}$ and $t\bar{t}$ pairs. For an intermediate mass Higgs, none of them however is competitive with Drell-Yan or Z_0-exchanges, which thus remains an insurmountable obstacle to the detection of the Higgs boson in this channel.

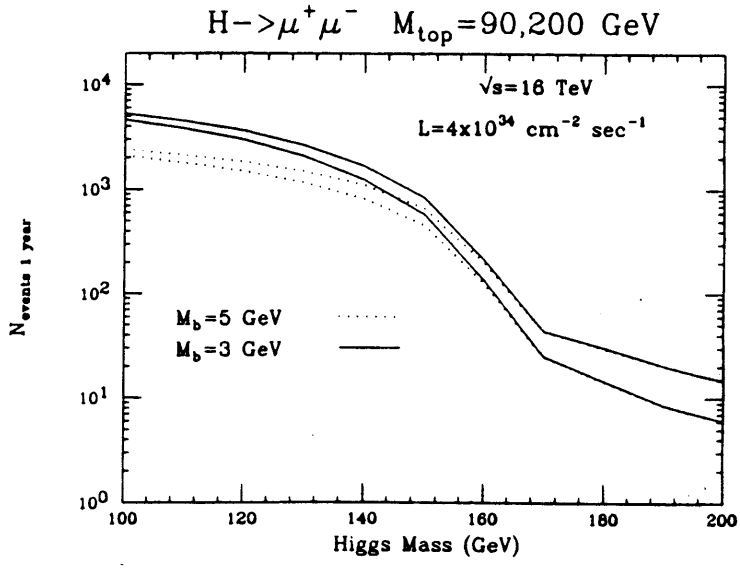

Fig. 14 Number of events in 1 year (10^7 sec) at a high luminosity machine with $\sqrt{s} = 16$ TeV for $pp \to gg + X \to H + X \to \mu^+\mu^- + X$. Branching fractions are calculated with$m_b = 3$ and 5 GeV.

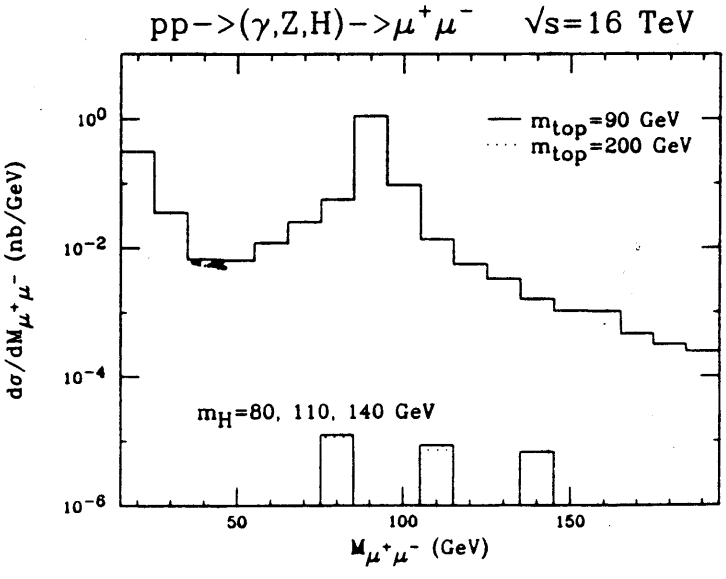

Fig. 15 Invariant mass distribution for $pp \to gg + X \to H + X \to \mu^+\mu^- + X$ compared with the irreducible physics background from Drell-Yan and Z_0 production. For Higgs production, we plot $\sigma_{H\to\mu^+\mu^-}/(10GeV)$, where σ is the total production cross-section for a Higgs boson decaying in μ-pairs.

4.2 $H \to \gamma\gamma$

In the mass region between the Z_0 mass and the 2 W-threshold, the dominant Higgs decay process (of the ones here under consideration) is that into two photons. Cross-sections and number of events, as one can see from **Fig.16** are therefore adequate,

as it was the case for the 2 μ channel, and the question is that of background and experimental resolution. It should be noticed that in this case, the experimental resolution constraint is particularly severe, because of the large number of π^0 produced with large p_t, and which can then decay into two photons. This background can be eliminated through the use of a position detector in conjunction with vertex localization[32]. Here we concentrate our attention to the background constituted by prompt γ-pairs from $q\bar{q}$ annihilation.The differential cross-section in the invariant mass of the photon pair is shown in **Fig. 17** together with the signal. The same considerations as for the μ-pair case apply here : the Higgs boson is very narrow in this region and the only meaningful comparison is with the total Higgs-cross-section in this channel, divided by the expected experimental resolution. Gamma detectors have a better experimental resolution than the μ detectors and we have chosen $\Delta E = 1\ GeV$. We see that for photon pairs with an invariant mass until 140 GeV, and with $cos\theta_\gamma \geq 0.5$, the signal at LHC is $\approx 10 \div 20\%$ relative to the background . Given the good statistical significance ($S/\sqrt{B}$ ratio)this channel can be considered as a good candidate for Higgs searches below the two W threshold[33].

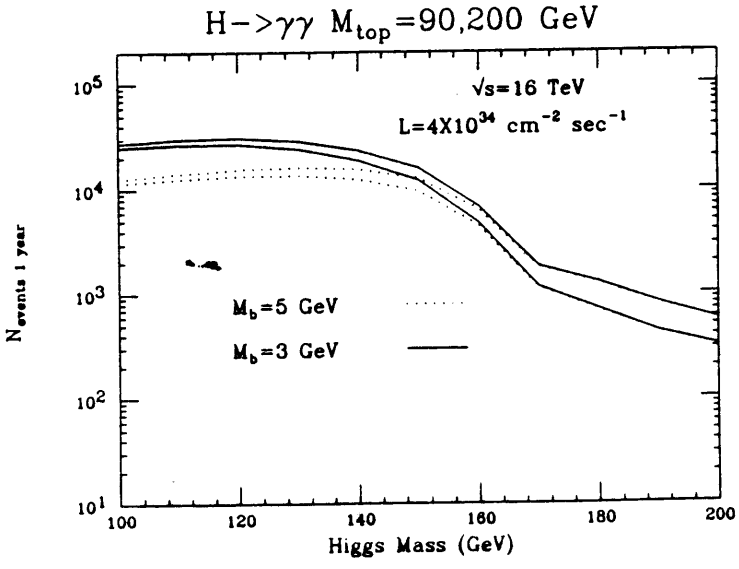

Fig. 16 Number of events in 1 year (10^7 sec) at a high luminosity machine with $\sqrt{s} = 16$ TeV for $pp \rightarrow gg + X \rightarrow H + X \rightarrow \gamma\gamma + X$, $\sqrt{s} = 16$ TeV. Branching fractions are calculated for bottom quark mass values 3 (full line) and 5 GeV (dots). Area between curves correspond to $90\ GeV \leq m_{top} \leq 200\ GeV$.

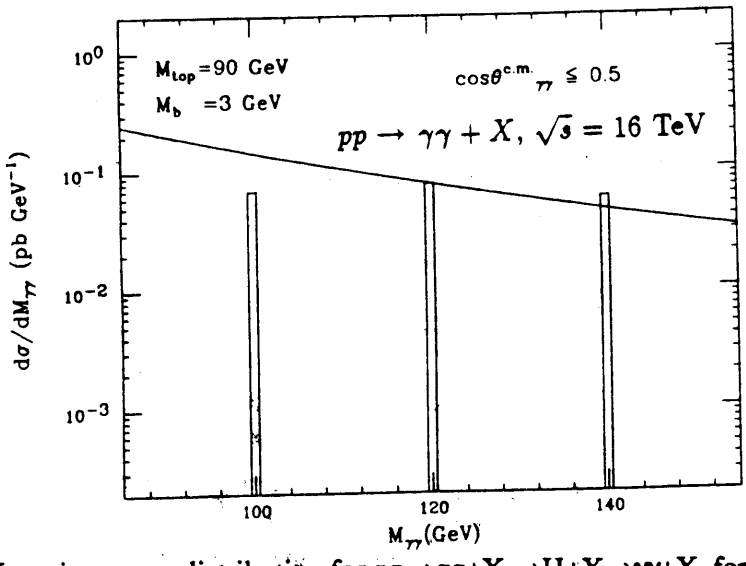

Fig. 17 Invariant mass distribution for pp→gg+X →H+X→γγ+X, for σ (H→γγ)/ΔE, ΔE=1 GeV, and for the irreducible QCD background

4.3 Higgs Detection in the 4μ Channel

The cross section for this process can be written as[34]

$$\frac{d\sigma(pp \to gg + X \to H + X \to 4\mu + X)}{dM dQ_1 dQ_2 dy} = MG(\sqrt{\tau}e^{y}, M_H^2)G(\sqrt{\tau}e^{-y}, M_H^2)\frac{G_F\pi}{16\sqrt{2}}$$

$$\left(\frac{\alpha_s}{\pi}\right)^2 |\eta_{gg}|^2 \frac{M_H\Gamma_H}{\pi D_H}\frac{p^*}{\Gamma_H}\frac{G_F}{8\pi\sqrt{2}}\frac{Q_1^3Q_2^3}{M_H^2 D_1 D_2}\left(\frac{\Gamma_Z m_Z}{\pi}\right)^2 (B_{Z\to\mu^+\mu^-})^2 C(Q_1^2, Q_2^2, M^2) \quad (4.5)$$

where

$$C(Q_1^2, Q_2^2, M^2) = 4\frac{2Q_1^2Q_2^2 + (Q_1 \cdot Q_2)^2}{Q_1^2Q_2^2} \quad (4.6)$$

and $|\eta_{gg}|^2$ is the usual integral over the triangle diagram.Also

$$D_H = (M^2 - M_H^2)^2 + M_H^2\Gamma_H^2 \quad (4.7)$$

In the region where the Z_0's are off the mass shell, the Higgs boson is extremely narrow, and one can use the narrow width approximation to estimate the cross-section. On the other hand, above the two IVB threshold , the Higgs has an increasingly large width and it is necessary to keep the propagator. In this region however the two Z_0's are on the mass shell and one can use the delta function approximation for the Z_0 propagators. We show in **Fig.18** the Higgs boson production cross section and subsequent decay into 4μ's in the region below and around the two Z_0's threshold, for different values of the top mass, at the energy $\sqrt{s} = 16TeV$. We notice in this figure two interesting features : a drop in the cross section at $M_H = 2m_W$ due to the opening of the W^+W^-threshold (reflecting the drop in the branching fraction) and the peaking of the cross-section for $\frac{4m_{top}^2}{M_H^2} \approx 0.7$

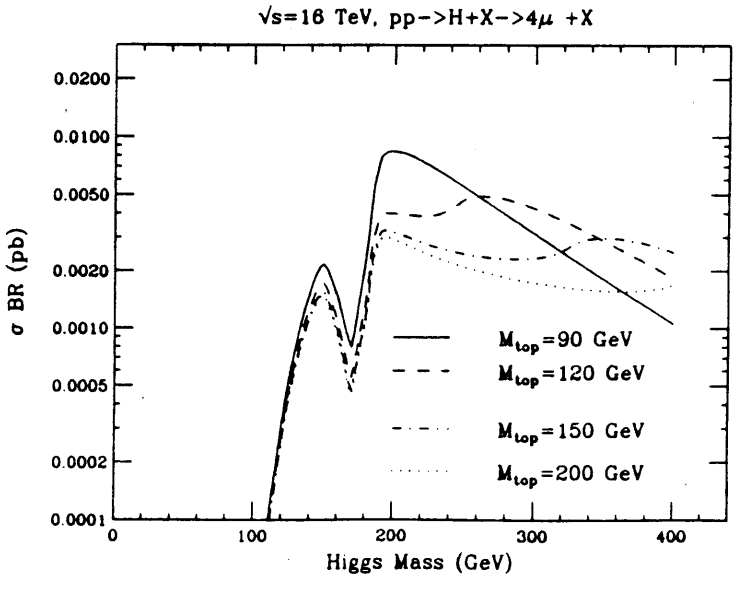

Fig.18 Production cross-section for

$$pp \to H + X \to Z_0^* Z_0^* + X \to (\mu^+\mu^-)(\mu^+\mu^-) + X$$

at $\sqrt{s} = 16TeV$ for different values of m_{top}

We can now see in detail the mass distributions of the two muon pairs resulting from the decay of the Z^0's. Using Eq. 2.21, we show in **Fig.19** a scatter plot of the invariant mass distribution of one muon pair versus the other. We have chosen to do

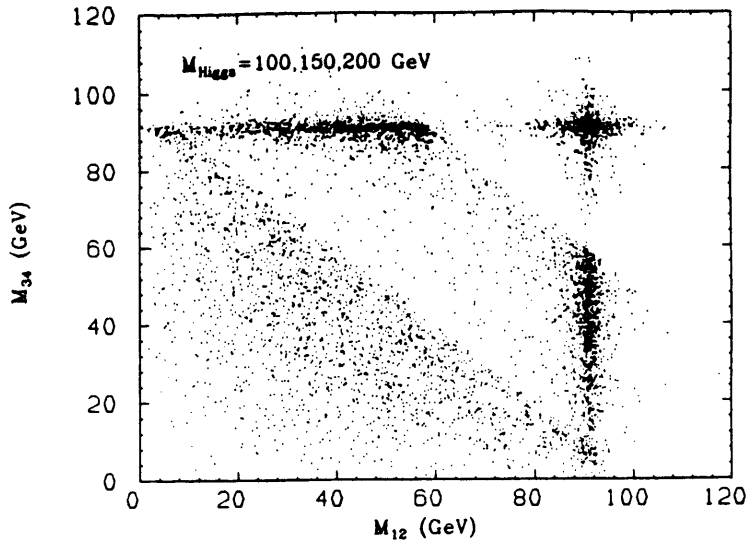

Fig. 19 Phase space population of the invariant mass regions for two μ-pairs from the decay $H \rightarrow Z_0^* Z_0^* \rightarrow \mu_1^+ \mu_2^- \mu_3^+ \mu_4^-$ for $M_{Higgs} = 100, 150, 200$ GeV,respectively.

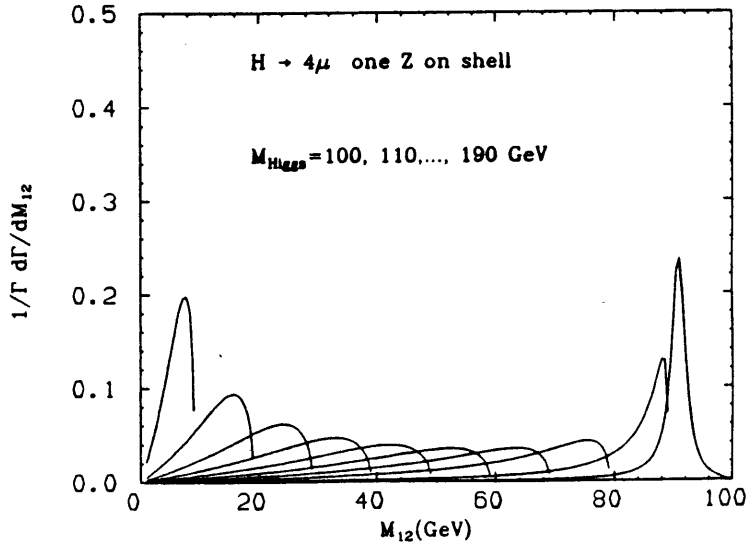

Fig. 20 Normalized probability distribution for the process $H \rightarrow Z_0 Z_0^* \rightarrow \mu_1^+ \mu_2^- \mu_3^+ \mu_4^-$ with $M_{Higgs} = 100, 110, 120, 130, 140, 150, 160, 170, 180, 190$ GeV.

so for three different values of the Higgs mass, i.e. M_H =100, 150 and 200 GeV, so as to clearly illustrate the transition from the region where both Z^0's are off the mass-shell to the one where they are both produced on-the-mass shell. These scatter plots emphasize that the search for the Higgs boson in the mass region $m_Z \leq M_H \leq 2m_Z$ can in principle be triggered by looking for one real Z^0. Let us then use Eq. 2.21 with one Z^* always on the mass shell and study the spectrum of the other pair. By using the narrow width approximation in Eq. 2.21 for one Z_0, we look at the structure of the other μ-pair for different values of the Higgs mass. This is shown in **Fig.20** where the peak one observes in the μ-pair invariant mass corresponds to the values $M_{\mu^-\mu^+} = M_H - m_Z$.

All the above plots reflect the same physical point, i.e. that one can look for the

Higgs boson in the region $130 \div 170\ GeV$, imposing the presence of at least one Z^0, without appreciable loss of signal [35].

In general, in hadronic collisions there are scores of strongly produced μ pairs. The spectrum of these μ pairs is in general quite different from the one we are discussing here, since the Z_0 propagators pull the mass of the lepton pairs towards the highest value allowed by phase space. Cuts on the invariant mass of the μ-pair will then reduce this background. Alternatively one can study the signal in eletron and positron pairs. Neither of the previous suggestions however can eliminate the background constituted by Z_0-pairs of QCD origin. In the region above the two IVB threshold this background has been extensively studied and shown to be well below the signal until $M_H \leq 700GeV$ at the LHC/SSC[31]. On the other hand, the studies of this background in the lower region, the so called "intermediate Higgs" regime, are not yet complete. In this region, we have background contributions from the following processes :

$$q\bar{q} \rightarrow Z_0^* Z_0^* \rightarrow (\mu^+\mu^-)(\mu^+\mu^-) \tag{4.8}$$

$$q\bar{q} \rightarrow Z_0^* \gamma^* \rightarrow (\mu^+\mu^-)(\mu^+\mu^-) \tag{4.9}$$

and

$$gg \rightarrow Z_0^* Z_0^* \rightarrow (\mu^+\mu^-)(\mu^+\mu^-) \tag{4.10}$$

or

$$gg \rightarrow Z_0^* \gamma^* \rightarrow (\mu^+\mu^-)(\mu^+\mu^-) \tag{4.11}$$

where Z_0^* is a Z_0-boson either on or off the mass-shell. We have not listed processes with two virtual photons in the final state, since searching inclusively for at least one μ-pair with an invariant mass around theZ_0 would make these processes not important.

Although processes 4.10 and 4.11 are of higher order in the strong coupling constant α_s, the large gluon densities in the x-values of interest make these processes comparable in magnitude to q-$\bar{q}$ annihilation. In other words, the logarithmic growth in the gluon densities compensates for the (inverse) logarithmic behaviour in α_s. Recent calculations by Glover et al.[31] for the case in which the two Z_0's are real have shown that the gluon-gluon processes contribute as much as 50-70 % of the q-$\bar{q}$ processes, in the collider energy region of interest, where these estimates are respectively for LHC and SSC . One can expect this ratioes to remain approximately the same also for production of Z-pairs below threshold, i.e. for processes 4.8 and 4.10, although as the Higgs mass decreases, the production of gluons over that of quarks is bound to increase further.

Let us star with the cross section for the process

$$pp \rightarrow q\bar{q} + X \rightarrow Z_0^* Z_0^* + X \rightarrow (\mu^+\mu^-)(\mu^+\mu^-) + X \tag{4.12}$$

to which there contribute the following graphs

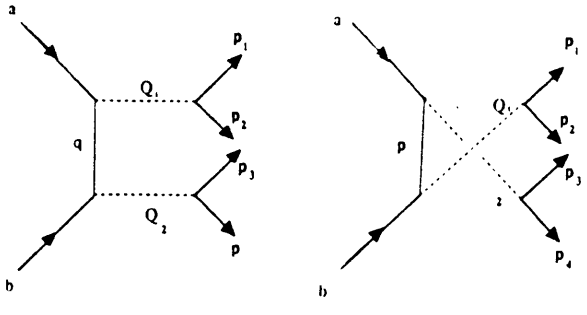

We should, in principle, consider the interference between processes (4.8) and (4.9), when the final states are the same.Their contributions however populate different regions of the phase space and we can discuss them separately.

The parton-parton cross-section for the above process can be written as

$$d^3\hat{\sigma} = \int_{4bodyLIPS} d\hat{\sigma} =$$

$$\frac{\pi p^*}{\hat{s}\sqrt{\hat{s}}}\frac{dz^*}{6}\left(\frac{m_Z\Gamma_Z}{\pi}\right)^2\frac{dQ_1^2}{(Q_1^2-m_Z^2)^2+m_Z^2\Gamma_Z^2}\frac{dQ_2^2}{(Q_2^2-m_Z^2)^2+m_Z^2\Gamma_Z^2}$$
$$\left(\frac{\Gamma_{Z\to\mu^+\mu^-}}{\Gamma_Z}\right)^2\frac{\alpha^2}{x_W^2(1-x_W)^2}(g_L^4+g_R^4)\frac{Q_1^2Q_2^2}{m_Z^4}B(\hat{s},\hat{t},\hat{u}) \qquad (4.13)$$

with

$$B(\hat{s},\hat{t},\hat{u}) = -Q_1^2Q_2^2\left(\frac{1}{\hat{t}^2}+\frac{1}{\hat{u}^2}\right)+\frac{\hat{u}}{\hat{t}}+\frac{\hat{t}}{\hat{u}}+\frac{2\hat{s}(Q_1^2+Q_2^2)}{\hat{u}\hat{t}} \qquad (4.14)$$

where the invariants of the parton-parton subprocess are given by

$$\hat{t} = Q_1^2 - \sqrt{\hat{s}}E_1 + p^*\sqrt{\hat{s}}z^* \qquad (4.15)$$

$$\hat{u} = Q_1^2 - \sqrt{\hat{s}}E_1 - p^*\sqrt{\hat{s}}z^* \qquad (4.16)$$

and $z^* = cos\theta^*$ with θ^* the parton-parton center of mass scattering angle. In the above equation , E_1 is the energy of one of the two Z_0, which is given by

$$E_1 = \frac{\hat{s}+Q_1^2-Q_2^2}{2\sqrt{\hat{s}}}$$

and p^* is the center of mass momentum of the final IVB's. It is easy to see that, in the narrow width approximation, the above expression reduces to the known one for production of two real Z_0's. One can also check that if one of two Z_0's is on the mass shell, our expression concides with the one obtained by Gunion, Kalyniak, Soldate and Galison[36].

We can obtain the hadronic cross-section for process (4.12) by folding the parton-parton cross-section of Eq. 4.13 with the parton densities. The cross-section then becomes

$$\frac{d\sigma(pp\to q\bar{q}+X\to Z_0^*Z_0^*+X\to 4\mu+X)}{dMdQ_1dQ_2dy} =$$
$$\sum_i(g_{Li}^4+g_{Ri}^4)F_i(\sqrt{\tau}e^y,M^2)F_{\bar{i}}(\sqrt{\tau}e^{-y},M^2)$$

$$\frac{4}{3}\frac{\pi p^*}{M^4}\frac{\alpha^2}{x_W^2(1-x_W)^2}(B_{Z\to\mu^+\mu^-})^2\frac{Q_1^3Q_2^3}{m_Z^4}\left(\frac{m_Z\Gamma_Z}{\pi}\right)^2\frac{1}{D_1D_2}\int_{-z_0}^{z_1}B(\hat{s},\hat{t},\hat{u}) \qquad (4.17)$$

If one requires that the outgoing vector bosons be always emitted within a given rapidity cut y_{cut}, the integration over the scattering angle gives

$$\int_{-z_1}^{z_0}B(\hat{s},\hat{t},\hat{u}) = -2Q_1^2Q_2^2\left[\frac{z_0}{(\sqrt{\hat{s}}E_1-Q_1^2)^2-\hat{s}p^{*2}z_0^2}+\frac{z_1}{(\sqrt{\hat{s}}E_1-Q_1^2)^2-\hat{s}p^{*2}z_1^2}\right]-$$
$$-2(z_0+z_1)+\frac{1}{\sqrt{\hat{s}}p^*}\left[2(\sqrt{\hat{s}}E_1-Q_1^2)+\frac{\hat{s}(Q_1^2+Q_2^2)}{\sqrt{\hat{s}}E_1-Q_1^2}\right]\cdot$$
$$\cdot\left[ln\frac{\sqrt{\hat{s}}E_1-Q_1^2+\sqrt{\hat{s}}p^*z_1}{\sqrt{\hat{s}}E_1-Q_1^2-\sqrt{\hat{s}}p^*z_0}+ln\frac{\sqrt{\hat{s}}E_1-Q_1^2+\sqrt{\hat{s}}p^*z_0}{\sqrt{\hat{s}}E_1-Q_1^2-\sqrt{\hat{s}}p^*z_1}\right] \qquad (4.18)$$

where z_1 and z_2 are defined as in sect.(3.4).

This expression should be directly compared with the one which describes the

same final state as obtained from gluon-gluon fusion into a Higgs boson.

We take a resolution $\Delta E = 10\ GeV$. In **Fig.21**, we show the differential cross section $\frac{d\sigma}{dM}$ as from Eq. 4.12 together with $\frac{\sigma_{H\to 4\mu}}{\Delta E}$, at the proposed LHC energy, for two different top mass values, and for both Z_0's produced with rapidity $|y| \leq 2.5$. We see that the signal is well visible above this particular background. Since the contribution coming from gluon-gluon fusion has been estimated to be as much as $50 \div 70\%$ of the one from quark annihilation, we can say that virtual Z_0 pairs of QCD origin do not constitute a dangerous background to direct Higgs production and detection in this region.

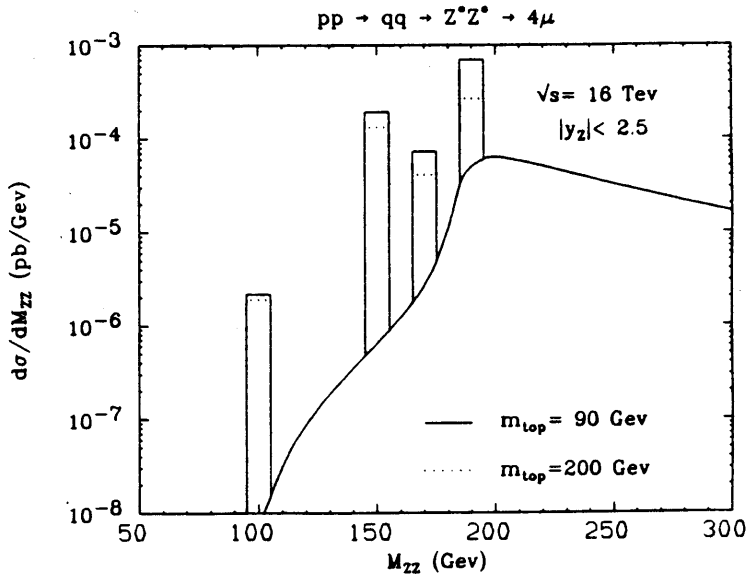

Fig.21 Differential cross section for $pp \to q\bar{q} + X \to Z_0^* Z_0^* + X \to (\mu^+\mu^-)(\mu^+\mu^-) + X$ (full line), and the total cross-section per 10 GeV for $pp \to H + X \to Z_0^* Z_0^* + X \to (\mu^+\mu^-)(\mu^+\mu^-) + X$.

4.3.1 Cross Section for $pp \to Z^0\gamma^* + X \to Z^0\mu^+\mu^- + X$

We now turn to the cross section for

$$pp \to Z_0\gamma^* + X \to Z_0 + \mu^+\mu^- + X \tag{4.19}$$

This process is peaked towards small values of the invariant mass of the non-resonant μ-pair and proceeds through $q\bar{q}$ annihilation as well as through gluon-gluon fusion. Since gluon densities in the range of interest are rather large at the LHC and SSC, the possibility that this contribution compares with that from $q\bar{q}$ has been investigated. We find that, unlike the case for Z_0-pair production, the gluonic contribution to $Z_0\gamma*$ processes is much smaller than the one from quark-antiquark annihilation. The physics reason for this difference is charge conjugation symmetry : the gluonic process proceeds via an intermediate quark loop for which only the vector part of the Z_0 coupling to quarks survives due to C-invariance. Because of this property, the gluon-gluon contribution is more than one order of magnitude smaller than the one from $q\bar{q}$ annihilation.

After integration over the two muon phase space, the differential cross-section for process (4.19) can be written as follows[37]:

$$\frac{d\hat{\sigma}}{d\hat{t}dk_1^2} = \frac{\alpha^2\alpha_s}{\hat{s}^2}\frac{8}{3}\left(\frac{1}{k_1^2}\right)\left(\frac{1}{4}\cdot\frac{1}{3}\right)Q_q^2(g_v^2+g_a^2)\left\{-M_Z^2k_1^2\left(\frac{1}{\hat{t}^2}+\frac{1}{\hat{u}^2}\right)+\frac{\hat{u}}{\hat{t}}+\frac{\hat{t}}{\hat{u}}+\frac{2\hat{s}(M_Z^2+k_1^2)}{\hat{u}\hat{t}}\right\} \tag{4.20}$$

where $\left(\frac{1}{4}\cdot\frac{1}{3}\right)$ is the initial spin and colour average factor.

A further integration over the parton structure functions will give us the contributions to the proton-proton cross section, namely

$$\frac{d\sigma}{dM_{Z\gamma^*}^2dk_1^2} = \frac{1}{s}\int_{-y_{cut}}^{y_{cut}} dy\left[\sum_{ij} f^i(x_1,Q^2)f^j(x_2,Q^2)\right]\frac{d\hat{\sigma}}{dk_1^2} \tag{4.21}$$

where

$$x_1 = \sqrt{\frac{\hat{s}}{s}}\,e^{y}, \qquad x_2 = \sqrt{\frac{\hat{s}}{s}}\,e^{-y} \qquad and \qquad Q^2 = \frac{\hat{s}}{4}$$

with

$$\frac{d\hat{\sigma}}{dk_1^2} = \int_{-z_1}^{z_0}\frac{d\hat{\sigma}}{dz^*dk_1^2} = \int_{-z_1}^{z_0}\frac{\lambda^{1/2}(\hat{s},m_Z^2,k_1^2)}{2}\frac{d\hat{\sigma}}{d\hat{t}dk_1^2}$$

and $z^* = cos\theta^*$, θ^* being the parton-parton center of mass scattering angle. We do not report here the analytical expression for the gluonic contribution, since it is rather cumbersome and can be found in ref [38], but only show the numerical results.

We have computed the invariant mass distribution of the two final leptons for different values of $M_{Z\gamma^*}$ at LHC energies using the Duke and Owens parton distribution functions with $\Lambda = 0.2$ Gev [39]. We show in **Figs.22** the contribution for a rapitity cut of 2.5 . As we have already mentioned the gluonic contribution is much smaller,

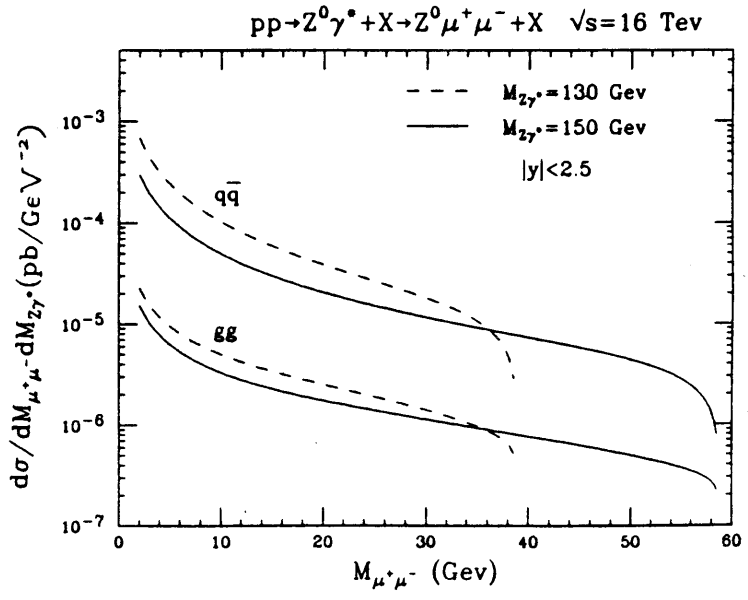

Fig.22 Differential cross-section for $pp \to Z^0\gamma^* + X \to Z^0\mu^+\mu^- + X$ at $\sqrt{s} = 16$ Tev. $q\bar{q}$ and *gluon gluon* contributions are shown separately for two different values of $M_{Z\gamma^*}$: 130 Gev (dashed line) and 150 Gev (full line).

both at the SSC and at the LHC energy . This is due to the fact that there is no contribution of the axial coupling to the box diagram for this particular process and that the axial coupling is larger than the vector coupling.

Here we are interested in the cuts to be imposed to the invariant mass of the non-resonant muon pair so that the insidious contribution from virtual photons can be eliminated. For this we compare the differential cross-section for a $\mu^+\mu^-$ pair

produced from $H- > Z_0Z^*$ and that from a $\mu^+\mu^-$ pair produced from $H- > Z_0\gamma^*$ as well as from $H- > Z_0Z^*$. We plot differential cross-sections in the non-resonant μpair for a Higgs signal at 130 and 150 GeV and integrate the background over a $M_{Z\gamma^*}$ bin of 5 and 10 Gev around this mass value. The result is shown in **Figs.23a-b** together with the signal.

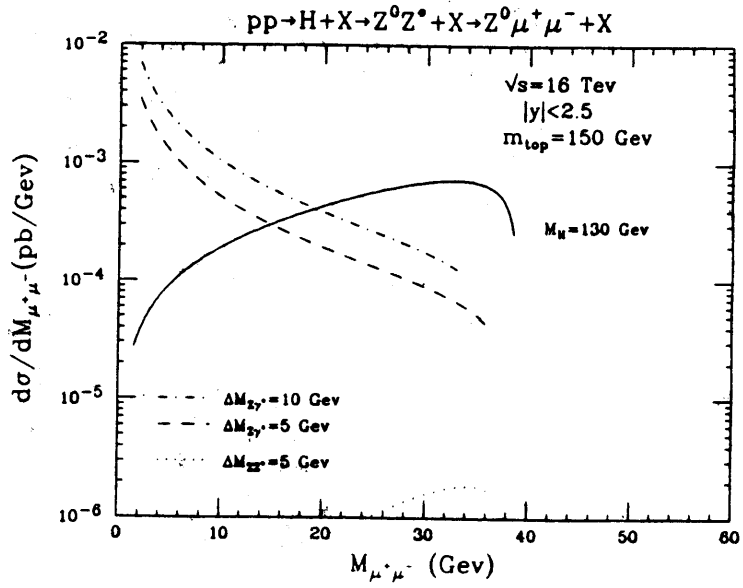

Fig.23a $\mu^+\mu^-$ invariant mass distribution for $pp \rightarrow H + X \rightarrow Z^0Z^* + X \rightarrow Z^0\mu^+\mu^- + X$ for $M_H = 130$ Gev (full line). Also shown are the contributions of $q\bar{q}$ background integrated over a $M_{Z\gamma^*}$ interval of 5 and 10 Gev around $M_{Z\gamma^*} = M_H$.

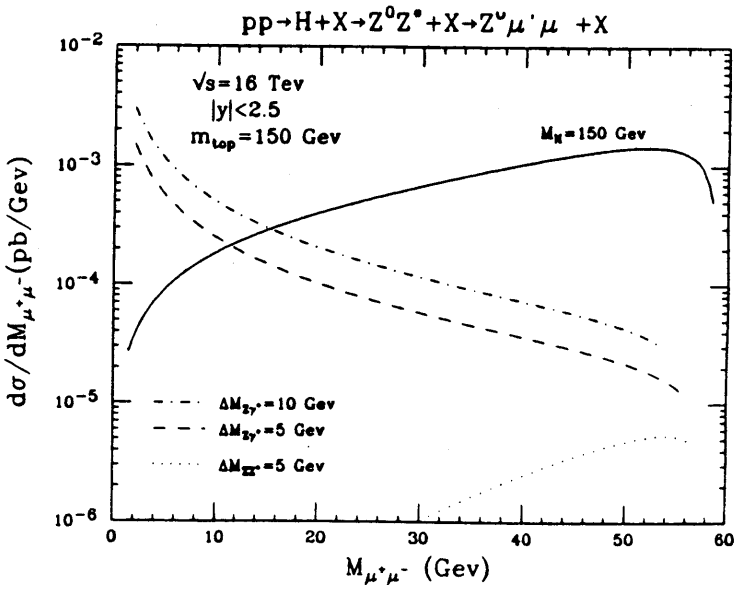

Fig.23b Same as fig.23a for $M_H = 150$ Gev.

We see that a cut of 15-20 Gev in the invariant mass of the $\mu^+\mu^-$ pair, will reduce considerably the background. Notice that also the signal will be reduced, however . Indeed this reduction will place limits on the range of Higgs masses for which the 4 lepton channel can give an acceptable signal to background ratio. We show in **Fig.24** the probability that, in the decay of a Higgs boson into Z^0Z^* , the two leptons from the off-mass-shell Z have an invariant mass larger than 10, 20 or 50 GeV. This plot shows that with a cut of 20 GeV on the non-resonant lepton pair, the signal for a Higgs boson of 130 GeV is reduced by 50% relative to the one for Z^*Z^* . Since the

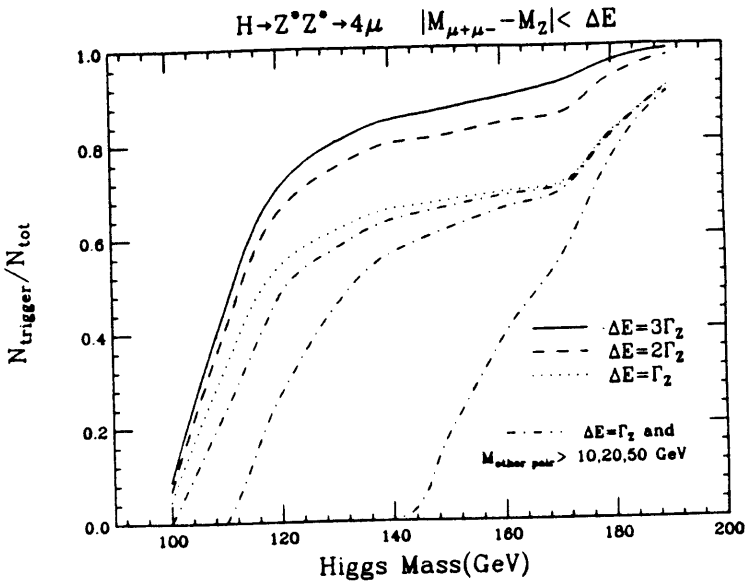

Fig.24 Probability that in the decay $H \rightarrow 4\mu$ the invariant mass of a μ-pair is larger than 10, 20 or 50 Gev (dot-dashed line), the other two muons being constrained to have an invariant mass close to M_Z.

total number of events in two lepton pairs at LHC for a Higgs boson of mass 130 GeV is $\approx$ 100-150 events, this confirms previous estimates [1, 35] that this channel cannot be used for Higgs boson masses less than 130 GeV.

4.4 Z_0-H Associated Production and Detection into $\mu^+\mu^-\gamma\gamma$

This process has a much smaller cross-section than the ones we have discussed so far. The interest in this production process lies in the possibility, as we shall see, of observing a Higgs boson with mass around that of the Z^0 , a region inaccessible to existing or presently planned electron-positron machines , because of luminosity, and very difficult to access with LHC or SSC because of background problems. A Higgs boson in this region has the highest decay probability in the photon photon channel, as far as electromagnetic and electroweak decays are concerned. The background to this process is constituted by QED higher order processes accompanying Z_0 production. As one can see from **Fig.13**, inclusive Z_0 production has a cross-section which is more than four orders of magnitude bigger than the one in which one Higgs boson is also produced. If we include branching ratioes, the cross-sections become unconfortably small. The question is then again that of signal versus background. Given the much larger production cross-section for inclusive Z_0 relative to the one associated with a Higgs boson, we can expect photon bremsstrahlung from the initial quark legs to constitute a non-negligble background. A detailed study of $Z_0\gamma\gamma$ production, based on the results of ref. [40], has recently been undertaken by T.Han. We show here some of his results. The invariant mass distribution of the photon pair accompanying Z_0 production is shown in **Fig.25**, together with the signal from HZ production. We have selected only large p_t ($\geq$30 GeV) photons, and used an an energy resolution for the signal such that$\Delta E_{\gamma\gamma}$ = 1 GeV at $M_H = 100GeV$: the signal is visible above the background, and can be improved with additional cuts. Such cuts can be imposed to the total (vector sum) transverse momentum distribution of the photon pair. Without any cut on the two photon mass, but only on the transverse momentum of the individual photons, one obtains the transverse momentum distribution shown in **Fig.26** . In this figure we have also shown the transverse momentum of the two

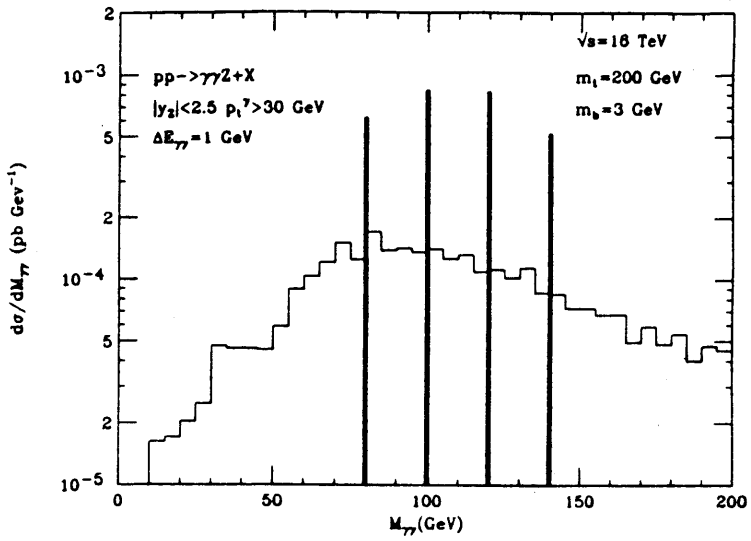

Fig. 25 Invariant mass distribution of two photons accompanying Z^0 production at $\sqrt{s} = 16$ TeV. Histogram is from QED bremsstrahlung from initial$q\bar{q}$ annihilation, narrow line from $\frac{\sigma^{incl}_{HZ\to\gamma\gamma Z}}{\Delta E}$ with ΔE the expected photon energy resolution.

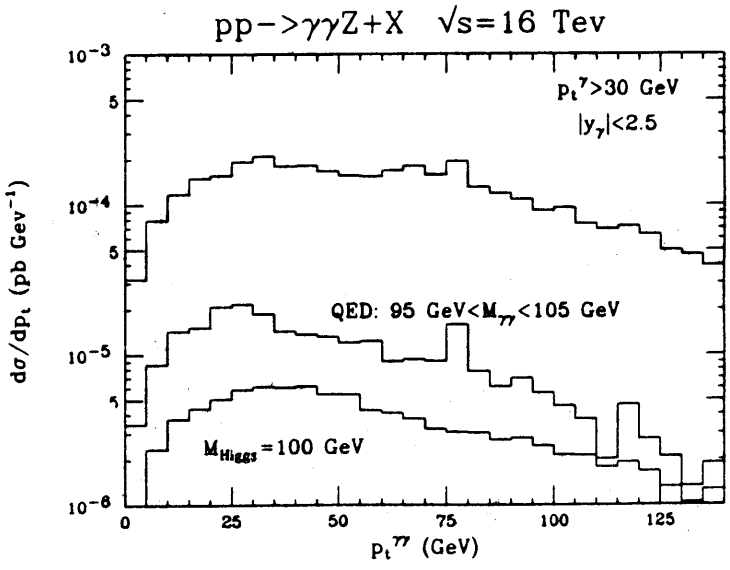

Fig. 26 Transverse momentum distribution of photon-pair from Higgs decay (lowest), QED bremsstrahlung with and without (highest) cuts with cuts on two photon invariant mass.

photons from Higgs decay, both without and with a cut on the two photon invariant mass.

The total number of events at LHC and SSC in the mass region of interest is then shown in Table I : the number is small, but at least at the LHC with high luminosity option, it may be sufficient[26].

M_{Higgs}	# Events $p_t^\gamma \geq 30GeV$ # Events $p_t^\gamma \geq 20GeV$	
80 GeV	19	31
100 GeV	25	34
120 GeV	25	30
140 GeV	16	17

We have not discussed associated production of W and Higgs bosons[41]. This process has a larger number of events than ZH production and an irreducible background from QED bremmstrahlung accompanying W production, similar to the one discussed above. However, we do not consider this signal as background free from other processes, as HZ is, since, at hadron colliders, W bosons are produced in scores through strong single top and $t\bar{t}$ production. Recent suggestions by Gunion [27] to use associated $t\bar{t}H$ production in the Z_0 mass region, encounters, we believe, the same difficulty.

5 Conclusions

In this talk we have discussed rates and event signatures for a Higgs boson in the 100-200 Gev mass region. It is shown that Higgs decay into four leptons has an acceptable signal with good discovery potential for $M_H \geq 130$ GeV. For a lighter Higgs, decay into two photons provides an unmistakeable signature. Direct Higgs production for $100\ GeV \leq M_H \leq 140\ GeV$ has an acceptable number of events, even in the presence of cuts, and with a conservative luminosity option. For lower M_H, the signal to background ratio may be unacceptably small and the extremely rare $HZ \rightarrow \gamma\gamma\mu^+\mu^-$ process is proposed for Higgs searches the Z_0 mass. In this case the small number of events requires an extremely high luminosity i.e. $4x10^{34} cm^{-2} sec^{-1}$ at $\sqrt{s}$ =16 GeV.

References

[1] C.Rubbia, "Perspectives for a Hadron Collider in the LEP Tunnel", CERN Seminar, November 6th, 1989.

[2] CDF Collaboration, F.Abe et al., Phys. Rev. Letters 64, 142 (1990); ibid. 147 (1990).
K. Sliwa, report to Rencontre de Moriond 1990.

[3] ALEPH Collaboration, Phys. Letters 236 (1990) 233.
OPAL Collaboration, Phys. Lett. 236 (1990) 225

[4] J.F.Gunion, H.E.Haber, G.L.Kane and S.Dawson, *The Higgs hunter's guide*, Frontiers in Physics Lecture Note Series. Addison Wesley 1990.

[5] S.L.Wu et al., ECFA Workshop on LEP200, eds A.Bohm and W.Hoogland, Vol. ii (1987).

[6] B.Cox and F.Gilman, p.87, Proc. 1984 Summer Study on Design and Utilization at SSC, eds. R.Donaldson and J.Morfin, American Physical Society.

[7] D. Froidevaux in Proceedings of the Workshop on Physics at Future Accelerators, ed. J.Mulvey, CERN 87-07 (1987).

[8] J.Ellis and G.L.Fogli, Physics Lett. 232B, 139 (1989);Phys.Lett. B249 (1990) 543.

[9] J.Ellis, M.K.Gaillard and D.V.Nanopoulos, Nucl. Phys. B106 (1976) 292.

[10] Z.Kunszt, Nuclear Physics B247 (1984) 339.

[11] M.Drees and K.Hikasa, Phys. Lett. B240 (1990) 455.

[12] S.C.Gorishny, A.L.Kataev, S.A.Larin and L.R.Surguladze, "Corrected three loop QCD correction to the correlator of the quark scalar currents and $\Gamma^{tot}(H^0 \rightarrow hadrons)$", TIFR/th/90-9, Feb. 1990.

[13] V. Barger, H. Baer and R.J.N. Phillips, Phys. Rev D30 (1984) 947.

[14] I. Bigi, Y. Dokshitzer, V. Khoze, J. Kuhn and P. Zerwas, Phys. Lett. 181B (1986)157.

[15] S. Geer, G. Pancheri and Y.N. Srivastava, Phys. Lett.192B (1987) 223.

[16] A.Grau, G.Pancheri and R.J.N.Phillips, Phys.Lett.B251 ((1990) 293.

[17] F. Wilczek, Phys. Rev. Lett. 39 (1977) 1304.
J.Ellis, M.K.Gaillard, D.V.Nanopoulos and C.T.Sachrajda, Phys. Lett. B83 (1979) 339.
T.G. Rizzo, Phys. Rev. D22 (1980) 178.
H.M.Georgi, S.L.Glashow, M.E.Machacek and D.V.Nanopoulos, Phys. Rev. Lett. 40 (1978) 692.

[18] A.I.Vainshtein, M.B.Voloshin, V.I.Zakharov and M.S.Shifman, Sov. J. Nucl. Phys. 30 (1979) 711.
L.B. Okun, *Leptons and Quarks* (North-Holland, Amsterdam, 1982).

[19] B.W.Lee, C.Quigg and G.B.Thacker, Phys. Rev. Lett.38 (1977) 883; Phys. Rev. D16 (1977) 1519.

[20] W.Y. Keung and W.J. Marciano, Phys. Rev. D30, 248 (1984).

[21] R.Cahn, Reports on Progr. in Physics 52 (1989) 389.

[22] E.Eichten, I.Hinchcliffe, K.Lane and C.Quigg, Rev. of Modern Phys. 56 (1984) 579; Erratum, ibidem, 58 (1986) 1065.

[23] R.Cahn, Nuclear Physisc B255 (1985) 341 ;
Erratum, ibidem, B262 (1985) 744.

[24] R.Cahn and S.Dawson, Physics Letters 136B (1984) 196;
Erratum, ibidem, 138B(1984) 464.

[25] J.D.Bjorken, *Proceedings of Summer Institute on Particle Physics*, SLAC-198, 1977. Ed. M.Zipf.

[26] A.Grau, G. Pancheri and T.Han, in Proceedings of the ECFA Large Hadron Collider Workshop, Aachen, 4-9 October 1990.

[27] J.F. Gunion, UCD-91-2.

[28] For an estimate of the inclusive Z_0 production at LHC see G.Altarelli, K.Ellis and G. Martinelli, Zeit Phys. C 27, 617 (1985).

[29] B.W.Lee, C.Quigg and G.B.Thacker, Phys. Rev. Lett. 38 (1977) 883; Phys. Rev. D16 (1977) 1519.
M.Chanowitz and M.K.Gaillard, Phys. Lett. 142B (1984) 85; Nucl. Phys. B261 (1985) 379.

[30] S. Dimopoulos, in Proceedings of the ECFA/LHC Workshop, Aachen, 4-9 October 1990.

[31] E.W.N.Glover and J.J.Van der Bij, Nucl. Phys. B231 (1989) 561.
E.W.N.Glover and J.J.Van der Bij, Phys. Lett. B206 (1988) 701.

[32] C.Seez, in Proceedings of the ECFA Large Hadron Collider Workshop, Aachen, 4-9 October 1990.

[33] D.Froidevaux,"Experimental Review of the Search for the Higgs Boson", Proceedings of the EFCA/LHC Workshop, Aachen, 4-9 October 1990.

[34] A.Grau, G.Pancheri and Y.Srivastava, Physics Letters B247 (1990) 611.

[35] M.Della Negra et al., "Search for $H \to Z^* Z^* \to 4$ *leptons* at LHC", Proceedings of the EFCA/LHC Workshop, Aachen, 4-9 October 1990.

[36] J.F.Gunion, P.Kalyniak, M.Soldate and P.Galison, Phys. Rev.D34, 101 (1986).

[37] J.F.Gunion, G.L.Kane and J.Wudka, Nucl.Phys. B299, 231 (1988).

[38] A.Grau, G.Pancheri and Y.N. Srivastava, "$Z^0\gamma^*$ Production at Hadron Colliders", LNF-91/026(P), May 1991. Submitted to Phys.Rev.D.

[39] D.W.Duke and J.F.Owens, Phys. Rev. D30 (1984) 49.

[40] V.Barger, T.Han and R.J.N.Phillips, Phys. ReV D39,146 (1989).

[41] Z.Kunszt and J.Stirling, in Proceedings of the EFCA/LHC Workshop, Aachen, 4-9 October 1990.